Lattice Statistics in a Magnetic Field. I. A Two-Dimensional Super-Exchange Antiferromagnet

M. E. Fisher

Proceedings of the Royal Society of London. Series A, Mathematical and Physical Sciences, Vol. 254, No. 1276. (Jan. 19, 1960), pp. 66-85.

Stable URL:
http://links.jstor.org/sici?sici=0080-4630%2819600119%29254%3A1276%3C66%3ALSIAMF%3E2.0.CO%3B2-A

Proceedings of the Royal Society of London. Series A, Mathematical and Physical Sciences is currently published by The Royal Society.

Lattice statistics in a magnetic field
I. A two-dimensional super-exchange antiferromagnet

By M. E. Fisher

Wheatstone Physics Laboratory, King's College, London

(*Communicated by J. T. Randall, F.R.S.—Received* 20 *June* 1959)

The partition function of a two-dimensional 'super-exchange' antiferromagnet in an arbitrary magnetic field is derived rigorously. The model is a decorated square lattice in which magnetic Ising spins on the bonds are coupled together via non-magnetic Ising spins on the vertices. By use of the decoration transformation all the thermodynamic and magnetic properties of the model are derived from Onsager's solution for the standard square lattice in zero field. The transition temperature $T_t(H)$ is a single-valued, decreasing function of the field H. The energy and the magnetization are continuous functions of T for all magnetic fields; but the specific heat and the temperature gradient of the magnetization become infinite as $-\ln|T-T_t|$. The initial $(H=0)$ susceptibility is a continuous and smoothly varying function of T with a maximum 40 % above the critical point; but $\partial\chi/\partial T$ becomes infinite at $T = T_c$. In a non-vanishing field the susceptibility has a logarithmic infinity at $T = T_t$. For small fields the behaviour near the critical point is given by

$$\chi \approx (N\mu^2/kT)\{2-\surd 2-D(T-T_c)\ln|T-T_c|-D'H^2\ln|T-T_c|\},$$

where D and D' are constants.

Introduction

The Ising model, originally proposed as a model of ferromagnetism, is one of the simplest models of a co-operative physical assembly. None the less, its salient features are characteristic of many real systems and, furthermore, it is one of the few models for which rigorous mathematical results have been obtained. (For a review of the extensive literature see Newell & Montroll (1953).) Thus from the classic work of Onsager (1944) one knows precisely how the energy and specific heat of the two-dimensional quadratic lattice in zero magnetic field behave through the transition region. This knowledge has proved invaluable in estimating the reliability of approximate but more general methods such as those of Bragg & Williams, Bethe and, more recently, Kikuchi (1951).

Following Onsager's work exact partition functions have been obtained for a number of other plane lattices in zero magnetic field (Houtappel 1950; Syozi 1951; Fisher 1959*a*). Kaufman & Onsager (1949) were further able to calculate the pair correlations for the square lattice in zero field and Onsager (unpublished) and Yang (1952) derived the spontaneous magnetization or long-range order. On the other hand, no exact results have been found for any three-dimensional lattice and the partition functions of the two-dimensional lattices have not been evaluated in a finite magnetic field. In particular the susceptibility of the square lattice is unknown even in the limit of zero field. On the basis of approximate calculations it is generally agreed that the initial susceptibility of the ferromagnetic square lattice becomes infinite at the critical temperature more rapidly than predicted by the Curie–Weiss law $\chi \sim (T-T_c)^{-1}$. Recently the author (Fisher 1959*b*) has been able to show that the singularity is actually of the form $\chi \sim (T-T_c)^{-\frac{7}{4}}$. On the other hand, the precise behaviour of the initial susceptibility of the antiferromagnetic lattice has been a matter of speculation. Some of the conflicting predictions that have been made are illustrated diagrammatically by the graphs of χ against T in figure 1.

Experimentally, antiferromagnetic solids are characterized by a maximum† in χ at a temperature which, in the earlier experiments, seemed close to that at which the specific heat rose to a sharp peak (see figure 1*a* where T_c denotes the temperature at which the specific heat anomaly occurs). The approximations of Bragg & Williams and of Bethe (see, for example, Ziman 1951) predict that χ has a discontinuous

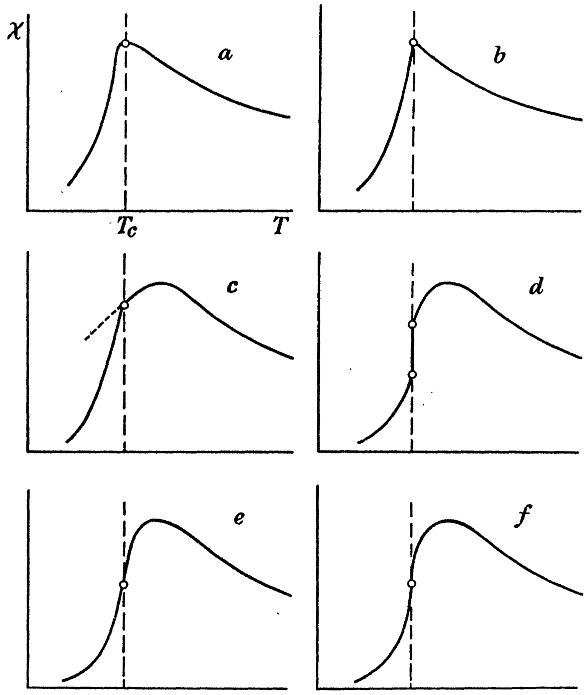

FIGURE 1. The zero-field susceptibility, χ, of an antiferromagnet as a function of temperature T, in the critical region according to (*a*) early experiments, (*b*), (*c*), (*d*) and (*e*) various approximate treatments, (*f*) recent experiments and the exact solution of the Ising model. T_c and dashed line denotes the position of the specific-heat anomaly and o denotes the corresponding value of χ. (Note that the curves are schematic).

gradient at T_c and falls away sharply on either side of T_c as in figure 1*b*. (In a magnetic field these approximations lead to a discontinuity in χ itself at T_t (Ziman 1951).) Brooks & Domb (1951) working with series expansions reached a similar conclusion (although their critical temperature was lower). More recently Domb & Sykes (private communication) concluded, from a study of higher terms in the series (Domb & Sikes 1957) that the susceptibility was of the form shown in figure 1*c*. Here the susceptibility passes through a maximum *above* T_c and is falling as T approaches T_c from above. At T_c a discontinuity in gradient was predicted with a possible meta-stable state extending below T_c. The Kikuchi (1951) approximation leads to similar conclusions (private communication from Mr D. M. Burley). Somewhat before this

† We refer here principally to $\chi_{||}$ the susceptibility parallel to the preferred axis.

Park (1956) had attempted to sum the susceptibility series on the assumption that they were algebraic like the spontaneous magnetization. His formulae gave the curves of figure 1*d* which also display a maximum above T_c. At T_c a discontinuity was predicted but Park observed that only small changes in the formulae were needed to make the curves join smoothly, with a continuous gradient as in figure 1*e*.

Sykes & Fisher (1958) using an analytic configurational approach discovered a way of writing the susceptibility as the sum of a dominant part which could be expressed in closed form in terms of the configurational energy, plus a residual series which appeared to be small at all temperatures. This suggested strongly that the susceptibility should have a similar anomaly to the energy, i.e. $\partial\chi/\partial T$ should become infinite as $-\ln|T-T_c|$ which implies a vertical tangent as indicated in figure 1*f*. Since then the author (Fisher 1959*b*) has been able to justify this conclusion rigorously by using Kaufman and Onsager's work on the correlations. (Incidentally this disproves Park's conjecture that χ is algebraic.) It is interesting to note that recent experiments on antiferromagnetic salts (see, for example, Lasheen, van den Broek & Gorter 1958 and Cooke, Lazenby, McKim, Owen & Wolf 1959) lead to curves rather similar to that in figure 1*f* and so in good accord with the true predictions of the Ising model.

The above results, however, do not yield explicit expressions for the initial susceptibility as a function of temperature, nor do they indicate how χ behaves in a finite magnetic field. In the present paper we discuss a two-dimensional model which fulfils these requirements. Thus we obtain an explicit formula for $\chi(T,H)$ (equation (30) below) which shows that in a finite field χ has a logarithmic singularity. Near the zero field critical temperature the behaviour is actually given by

$$\chi(T,H) \approx \frac{N\mu^2}{kT}\{\xi_c - D(T-T_c)\ln|T-T_c| - D'H^2\ln|T-T_c|\}$$

where ξ_c, D and D' are constants (see also figure 13 below). Exact expressions are also obtained for the energy, specific heat and magnetization of the model as functions of T and H.

1. Model of a super-exchange antiferromagnet

The model for which we obtain the results mentioned above is slightly different from the standard antiferrogmagnetic square Ising lattice which is treated by most authors. Consider the square array of Ising spins denoted by the black dots in figure 2, where each spin is supposed to have a magnetic moment μ through which it interacts with an external magnetic field H. We will also suppose that the magnitude of each spin is $S = \frac{1}{2}$ although this restriction can be removed. If coupling is introduced between these spins, such that nearest neighbours tend to aline with their spins pointing in opposite directions, then the lowest energy state will be one of antiferromagnetic ordering as indicated by the + and − signs in figure 2. When the temperature or magnetic field is increased from zero the order will break down and an order–disorder transition may occur at a given temperature or field. In the standard Ising model, antiferromagnetic ordering is achieved by introducing *direct* nearest-neighbour interactions between the spins of figure 2, so that parallel nearest-neighbour spins have a mutual potential energy $-J\,(J<0)$, whilst anti-parallel spins have an energy $+J$. As is well known this model exhibits a transition but rigorous results can only be obtained in a zero magnetic field.

Direct nearest-neighbour coupling is not the only way of achieving antiferromagnetic ordering. Indeed, the neutron diffraction experiments of Shull & Smart (1949) and their theoretical explanation by Anderson (1950) in terms of 'super-exchange' coupling show that in many real antiferromagnets the coupling between the magnetic spins takes place *indirectly* via a non-magnetic intermediary atom.

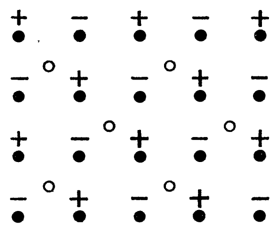

FIGURE 2. An antiferromagnetic array of Ising spins.

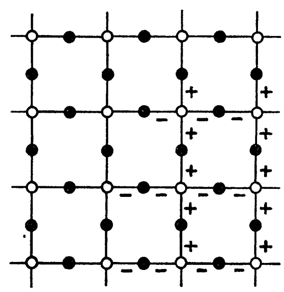

FIGURE 3. A super-exchange antiferromagnetic lattice. The black circles denote magnetic spins and the open circles non-magnetic spins. The vertical bonds are 'ferromagnetic', while the horizontal bonds are 'antiferromagnetic' in character.

We can construct a two-dimensional 'super-exchange' model along these lines by allowing the magnetic spins at the corners of a square in figure 2 to interact with each other via a non-magnetic central spin.† A 'non-magnetic' spin, which we denote by an open circle, is simply an Ising spin which is not coupled to the magnetic field, i.e. it has zero magnetic moment. To ensure antiferromagnetic ordering we must suppose that the magnetic spins marked by a + in figure 2 have a positive (ferromagnetic) interaction with their neighbouring non-magnetic spins, whilst those marked − have a negative (antiferromagnetic) interaction. If the resulting lattice is rotated through 45° it is seen to be quite equivalent to the 'decorated' square lattice shown in figure 3. This is a standard square Ising lattice with non-magnetic spins at the vertices which has been decorated by placing a magnetic spin on each bond. The antiferromagnetic character is ensured by supposing that the vertical bonds are ferromagnetic $(J>0)$, whilst the horizontal bonds are antiferromagnetic $(J<0)$. (Equivalently one may suppose that all the interactions are ferromagnetic, but that the magnetic moments of the spins decorating the horizontal

† A superficially similar but actually distinct type of 'super-exchange' Ising model was considered by Domb & Potts (1951).

bonds are of opposite sign to the moments of the spins on the vertical bonds: mathematically this convention is rather more convenient.)

The super-exchange model just described is clearly distinct from the usual antiferromagnetic Ising model. Notice, for example, that the standard model becomes ferromagnetic when the sign of J is changed, whereas the super-exchange model remains invariant. None the less, the super-exchange decorated lattice is a reasonable model of an antiferromagnet. Furthermore, its partition function can be calculated rigorously in an arbitrary magnetic field, thereby yielding explicit expressions for all the thermodynamic and magnetic properties of the lattice as functions of both temperature and magnetic field. This is achieved, as shown in § 2 below, by employing an algebraic transformation to relate the decorated lattice in a magnetic field to the standard square lattice in zero field. The properties of the super-exchange lattice then follow directly from Onsager's work. The details are presented in §§ 3 to 6 of the paper, whilst various generalizations of the model are discussed in § 7. By using the results of Kaufman & Onsager (1949) and of Yang (1952) it is also possible to calculate the long-range order and most of the spin-spin correlation functions of the super-exchange lattice. This is done in part II of the present paper which is being prepared for publication.

2. Derivation of the partition function

As noted above the super-exchange antiferromagnetic lattice of figures 2 and 3 is derived from the usual square-lattice Ising model by 'decorating' each bond of the standard lattice with an extra spin. Now the configurational partition function Z of any such decorated lattice may be derived from the corresponding partition function Q of the basic (undecorated) lattice by a simple transformation of the temperature and magnetic field variables ('bond decoration process'). The method has been used in particular applications by Naya (1954) and by Syozi & Nakano (1955). Recently the present author (Fisher 1959*a*) has discussed this and other transformations of the Ising model from a more general standpoint. Normally the bond decoration process connects a decorated lattice in a non-zero magnetic field to the corresponding basic lattice also in a non-zero field. For a certain class of decorated lattices, however, it was discovered that the partition function for a *finite* magnetic field could be derived from that of the basic lattice *in zero magnetic field*. In all such cases the resulting decorated lattice is anti-ferromagnetic in character, one of the simplest examples being the model under discussion. The general transformations for the partition function are given in the author's paper (Fisher 1959*a*), but it is worth while presenting the details for the present model, since the arguments are simple and will serve to introduce the notation.

We denote a spin variable of a non-magnetic or vertex spin of the antiferromagnetic decorated lattice (figure 3) by $s_i^0 = \pm 1$, that of a magnetic spin on a vertical bond by $s_j^+ = \pm 1$ and that of a magnetic spin on a horizontal bond by $s_k^- = \pm 1$. A configuration of a lattice of N vertices (and $2N$ magnetic spins) is then specified by the set of $3N$ spin variables s_i^0, s_j^+ and s_k^-. The corresponding energy is then taken to be

$$E = -J\Sigma s_i^0 s_j^+ + J\Sigma s_i^0 s_k^- - \mu H \Sigma s_j^+ - \mu H \Sigma s_k^-, \tag{1}$$

where J is the interaction energy between a neighbouring magnetic and non-magnetic spin and $J > 0$ for a ferromagnetic coupling, μ is the magnetic moment of the magnetic spins and H is the external magnetic field. The first two sums extend over the N vertical and N horizontal bonds, respectively, and the last two over the two sets of N magnetic spins. It is convenient to introduce the dimensionless parameters

$$K = J/kT, \quad \alpha = \mu H/2J, \tag{2}$$

and

$$L = \mu H/kT = 2K\alpha. \tag{3}$$

The temperature is measured by K, and α is the reduced magnetic field. The partition function of the decorated lattice may now be written

$$Z(K,L) = \sum_{s^0=\pm 1} \sum_{s_j^+=\pm 1} \sum_{s^-=\pm 1} \exp\{K\Sigma(s_i^0 s_j^+ + s_i^0 s_k^-) + L\Sigma s_j^+ - L\Sigma s_k^-\}, \tag{4}$$

where, for convenience, the sign of the (dummy) variables s_k^- has been changed. As mentioned in the Introduction this is equivalent to taking all the interactions as ferromagnetic and associating moments of opposite signs with the spins s_j^+ and s_k^-, respectively. Now consider the summation over a particular spin variable s^+ for a magnetic spin on a vertical bond. We may write

$$\sum_{s^+=\pm 1} \exp\{Ks^+(s_1^0+s_2^0)+Ls^+\} \equiv f\exp\{Gs_1^0 s_2^0 + L_V s_1^0 + L_V s_2^0\},$$

where the equivalent (undecorated) interaction parameter G is defined by

$$\exp 4G(K,L) = \frac{\cosh(2K+L)\cosh(2K-L)}{\cosh^2 L}, \tag{5}$$

the new magnetic parameter by

$$\exp 4L_V(K,L) = \cosh(2K+L)/\cosh(2K-L) \tag{6}$$

and the multiplicative factor by

$$f^4(K,L) = 2^4\cosh(2K+L)\cosh(2K-L)\cosh^2 L. \tag{7}$$

Precisely similar relations hold for a magnetic spin on a horizontal bond except that the corresponding new magnetic parameter L_H is identically equal to $-L_V$ (change L to $-L$ in (5), (6) and (7)). Consequently, when the summations over all the magnetic spin variables are performed, the magnetic contributions L_V and L_H at each non-magnetic vertex cancel identically so that (4) reduces to

$$Z(K,L) = f^{2N} \sum_{s^0=\pm 1} \exp\{G\Sigma s_i^0 s_j^0\} = [f(K,L)]^{2N} Q\{G(K,L)\}, \tag{8}$$

where $Q(G)$ is the zero-field partition function of a standard square Ising lattice of N spins with interaction energy $J^* = kTG$. Since the magnetic field is zero this partition function is known exactly from the work of Onsager (1944). (Onsager denotes the interaction parameter G by H.) The relation (8) shows that all the thermodynamic *and* magnetic properties of the antiferromagnetic decorated lattice can be derived directly from Onsager's solution.

3. Properties of the transformation and the transition curve

The transformation equation (5) can be regarded as mapping the antiferromagnetic decorated lattice at a temperature T ($\sim 1/K$) and in a magnetic field H ($\sim \alpha = L/2K$) on to the standard lattice in zero field at a modified temperature T^* ($\sim 1/G$). Now the critical temperature of the standard Ising lattice is determined by

$$\exp 2G_c = 1+\sqrt{2}. \tag{9}$$

Consequently, for the antiferromagnet this equation determines the transition temperature T_t (at which the long-range antiferromagnetic order disappears) as a function of magnetic field. The resulting transition curve is given by the implicit equation

$$\sinh 2K_t = (2+2\sqrt{2})^{\frac{1}{2}} \cosh 2K_t \alpha. \tag{10}$$

In zero field this yields

$$K_c = K_t(0) = \tfrac{1}{2}\cosh^{-1}(1+\sqrt{2}) = 0{\cdot}764285, \tag{11}$$

which corresponds to a critical temperature

$$T_c = 1{\cdot}30841(J/k). \tag{12}$$

This is about 40 % lower than the critical temperature of the normal square net as is to be expected in view of the smaller effective co-ordination number of the present model.

Equation (10), of course, may also be regarded as an equation for the 'transition field', α_t, as a function of temperature (the transition field being the magnetic field required to destroy the long-range order at a given temperature). At zero temperature this is equal to the 'critical field' $\alpha_c = 1$, or $H_c = 2J/\mu$, which, as may be seen by simple energetic arguments, is just strong enough to aline *all* the magnetic spins. As the temperature is raised the transition field changes and finally falls to zero at the critical point T_c, above which temperature no long-range ordering can occur. The actual relation is shown by the heavy curve in figure 4. In the shaded region below the transition curve or phase boundary, long-range antiferromagnetic ordering prevails with the magnetic spins on the vertical and horizontal bonds pointing predominantly in opposite directions. Outside the transition curve the behaviour is essentially paramagnetic.

At low temperatures the transition field falls away from its maximum value, $\alpha = 1$, linearly with temperature according to

$$\alpha_t = 1-\tfrac{1}{4}K^{-1}\ln 2(1+\sqrt{2})-O(\mathrm{e}^{-4K}/K). \tag{13}$$

This is at variance with the work of Brooks & Domb (1951) and of Ziman (1951). Brooks & Domb studied the normal antiferromagnetic square net by expansion methods and exposed the general features of the transition region as described above. However, they postulated that the linear term in (13) would vanish, making the transition curve horizontal at low temperatures. Ziman, on the other hand, used the Bethe approximation which indicated a positive (increasing) linear term so that the transition curve 'bulged' above the critical field $\alpha = 1$ and $T_t(H)$ became a doublevalued function of H. Ziman suggested that this was merely due to the inadequacy of the Bethe approximation and our present result confirms his view.

For small magnetic fields (higher temperatures) the transition temperature falls slowly from its maximum value T_c as the magnetic field is increased. From (10) we obtain the expansion

$$T_t(H) = T_c - \tfrac{1}{2}(2+2\sqrt{2})^{-\frac{1}{2}}(\mu^2/kJ)\,H^2 + O(H^4). \tag{14}$$

At $\alpha = \frac{1}{4}$, i.e. at a field of one-quarter the critical field, the transition temperature has only fallen by 4 %, whilst at $\alpha = \frac{1}{2}$ we find $T_t(\frac{1}{2})/T_c = 0{\cdot}8049$.

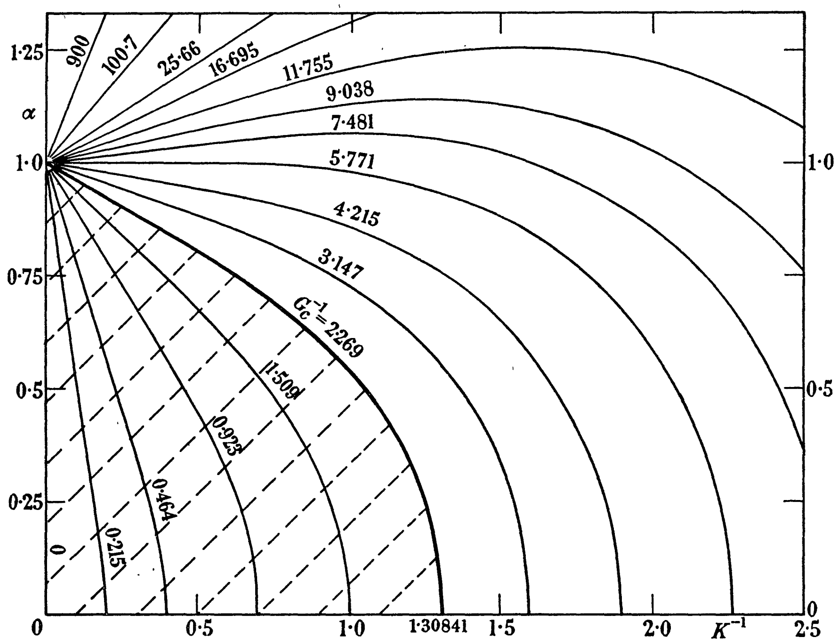

FIGURE 4. The transition curve and 'isotherms' of reduced magnetic field $\alpha = (\mu/2J)\,H$ against reduced temperature $K^{-1} = (k/J)\;T$ for fixed parameter G^{-1}.

The remaining (thin) curves in figure 4 represent the complete set of 'isotherms' obtained by fixing the value of G in the transformation equation (5). They are labelled by the modified temperatures, G^{-1}, of the corresponding square lattice and indicate how the various zero-field properties of the basic lattice are mapped on to the temperature-magnetic field plane of the decorated lattice. For large K (low temperatures) and near $\alpha = 1$ we have the generalization of (13), namely,

$$\alpha = 1 - \tfrac{1}{4}K^{-1}\ln\left(e^{4G}-1\right) + O(K^{-1}e^{-4K}), \tag{15}$$

which shows that the isotherm for $G^{-1} = 4/\ln 2 = 5{\cdot}77077$ has zero slope at low temperatures. (The critical isotherm corresponds to $G^{-1} = 2{\cdot}26919$.) In zero field the transformation simplifies to

$$G = \tfrac{1}{2}\ln\cosh 2K, \quad K = \tfrac{1}{2}\cosh^{-1}\ln 2G, \tag{16}$$

whilst for small fields and all temperatures we can obtain the expansion

$$K^{-1} = K_0^{-1} - \alpha^2\tanh 2K_0 + O(\alpha^4), \tag{17}$$

where K_0 is given by (16). At high temperatures (small K) and all fields the expansion is

$$G(K,\alpha) = K^2 - \tfrac{2}{3}K^4(1+6\alpha^2) + \tfrac{32}{45}K^6(1+15\alpha^2+15\alpha^4) + \ldots, \tag{18}$$

which shows explicitly that high temperatures always transform into high temperatures. At low temperatures, on the other hand, the results depend on the magnetic field. For zero field the relation is simply

$$G(K,0) = K - \tfrac{1}{2}\ln 2 + \tfrac{1}{2}\mathrm{e}^{-4K} + \ldots, \tag{19}$$

whilst if $0 < |\alpha| < 1$

$$G(K,\alpha) \simeq K(1-|\alpha|), \tag{20}$$

indicating that low temperatures transform to low temperatures. Near $|\alpha| = 1$ equation (15) is valid whilst for $|\alpha| > 1$ the relation is

$$G(K,\alpha) \simeq \tfrac{1}{4}\exp\{-4K(|\alpha|-1)\}, \tag{21}$$

so that, in this case, low temperatures on the decorated lattice transform to high temperatures on the basic lattice. (These general features of the transformation are evident from the curves of figure 4.)

4. Energy and specific heat

The configurational energy and specific heat of the antiferromagnetic lattice can be derived in the standard way by differentiating the partition function $Z(K,\alpha)$. It is convenient to define the reduced energy per vertex (i.e. per non-magnetic spin) by

$$\mathscr{U}(K,\alpha) = -U/NJ = N^{-1}\partial \ln Z(K,\alpha)/\partial K, \tag{22}$$

where U is the total configurational energy of the lattice. The reduced energy is always positive and varies from a maximum at $T = 0$ to zero at $T = \infty$. Through the transformation (8) we find

$$\mathscr{U}(K,\alpha) = (G_K)_\alpha \mathscr{U}^*(G) + 2\partial \ln f(K,\alpha)/\partial K, \tag{23}$$

where $(G_K)_\alpha$ denotes the derivative $(\partial G/\partial K)_\alpha$ and where $\mathscr{U}^*(G)$ is the reduced energy of the standard square net. From Onsager (1944) we have

$$\mathscr{U}^*(G) = \coth 2G\left[1 + (2\tanh^2 2G - 1)\frac{2}{\pi}K(k_1)\right], \tag{24}$$

where the modulus of the complete elliptic integral $K(k_1)$ is

$$k_1 = 2\tanh 2G/\cosh 2G. \tag{25}$$

By use of equations (5) and (7) we could, of course, rewrite (23) as an explicit function of K and α but the resulting formula is rather long. The main point is that (for $T > 0$) both $G(K,\alpha)$ and $f(K,\alpha)$ are continuous analytic functions of both arguments so that $(G_K)_\alpha$, $\partial \ln f/\partial K$ and all similar derivatives are smooth, slowly varying functions. For example, in zero field we have

$$(G_K)_\alpha = \frac{\partial}{\partial K}\ln f = \tanh 2K \quad (\alpha = 0). \tag{26}$$

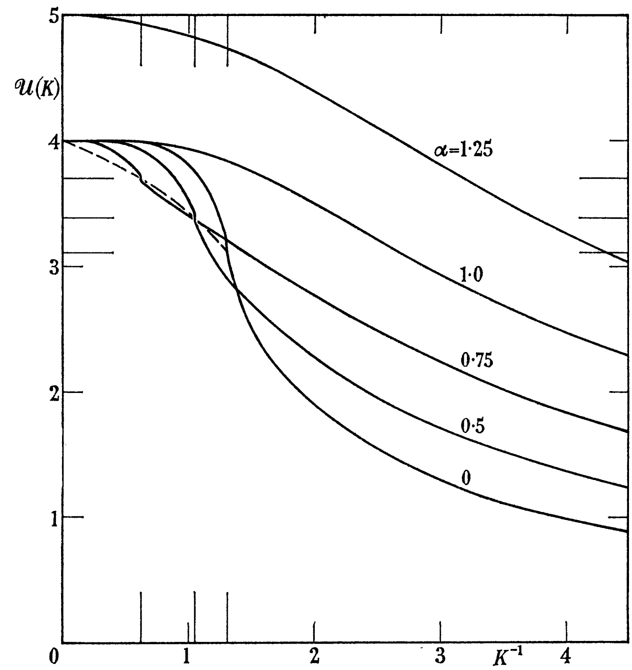

FIGURE 5. The energy of the super-exchange antiferromagnet as a function of temperature for fixed magnetic field. The dashed line is the locus of transition points and the critical co-ordinates are marked on the axes.

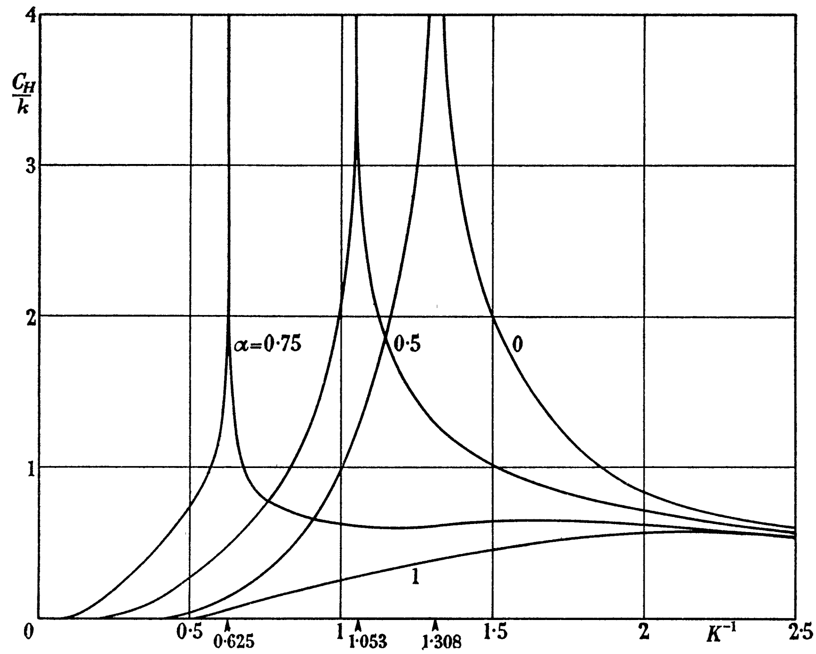

FIGURE 6. The specific heat C_H as function of temperature at fixed magnetic field.

(At zero temperature, that is in the limit $K \to \infty$, simple discontinuities occur at the critical field $\alpha = 1$. This can be seen from figure 4.) These considerations show that the behaviour of the energy in the transition region is determined by the elliptic integral term in (24). Thus the energy is continuous through the transition region and for fixed magnetic field behaves as $\mathscr{U}_t + A(T-T_t)\ln|T-T_t|$. In consequence C_H, the specific heat at constant field, becomes infinite as $-\ln|T-T_t|$. This type of singularity is characteristic of all plane Ising lattices for which exact solutions are known (see, for example, Houtappel 1950 and Syozi 1951). An expression for C_H is readily derived by differentiating (23) with respect to K. The result may be expressed directly in terms of Onsager's formula for the specific heat C^* (see equations (31) and (32) below).

The detailed behaviour of the thermodynamic functions can be seen from figures 5 and 6 in which the energy and the specific heat are plotted as functions of the temperature for various fixed magnetic fields. The specific heat anomaly is greatest in zero field, the strength of the singularity decreasing steadily as α increases and finally vanishing at the critical field $\alpha = 1$. The position of the infinity moves to lower temperatures as the field increases in accordance with the transition curve discussed in the previous section. At the critical field the energy, as T increases, falls slowly from the value $\mathscr{U}_0 = 4$. In smaller fields the drop is more rapid and the gradient becomes infinite at the appropriate transition temperature. In larger fields the ground state ($T = 0$) energy is greater than $\mathscr{U}_0$ and the curve falls slowly as for $\alpha = 1$. The critical value of the energy (in zero field) is given by

$$\mathscr{U}(T_c)/\mathscr{U}(0) = \tfrac{1}{2}(1+\surd 2)^{\frac{1}{2}} = 0{\cdot}77689,$$

which is slightly larger than the corresponding figure 0·70711 for the normal square lattice. With increasing field the transition energy $\mathscr{U}(T_t)$ increases and the locus of transition points meets the axis at

$$\lim_{T\to 0} \mathscr{U}(T_t) = \mathscr{U}_0 = 4.$$

At high temperatures the energy falls off as $\mathscr{U} \simeq 4K(1+\alpha^2)$.

Figure 7 shows the energy as a function of the magnetic field for fixed temperature. For fields greater than $\alpha = 1$ all spins are alined with the field and the energy rapidly becomes proportional to α. For smaller fields and below the critical temperature there is an anomaly at the transition field H_t of the form

$$\mathscr{U}_t + A'(H-H_t)\ln|H-H_t|.$$

The energy reaches a minimum at a slightly greater field. Figure 8 shows the contours of the energy surface in the temperature-field plane. The transition curve is marked by a dashed line and the energy contours touch this tangentially. The dotted line represents the locus of energy minima. It can be seen that for temperatures up to $T = 1{\cdot}45(J/k)$, i.e. 11 % higher than the critical temperature, the energy at first *decreases* when the magnetic field increases from zero. This is an indication of the residual intermediate-range order still present above the transition temperature.

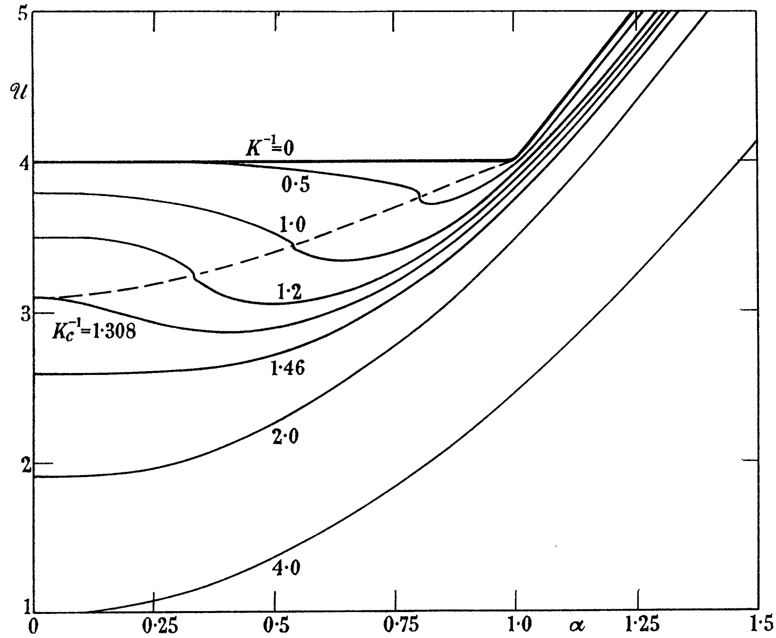

FIGURE 7. The variation of energy with magnetic field at fixed temperature. The dashed line is the locus of transition points.

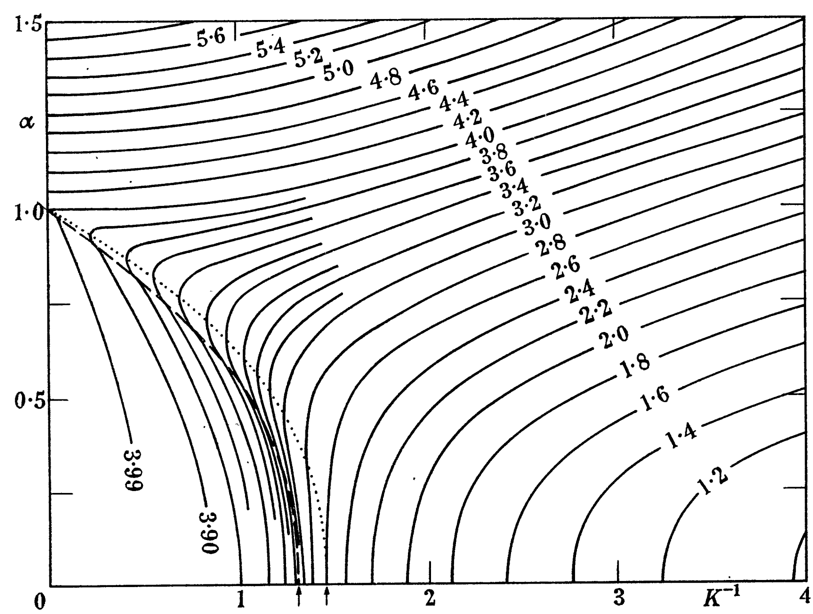

FIGURE 8. The contours of constant energy in the temperature-magnetic field plane. The dashed line is the transition curve and the dotted line is the locus of energy minima (at fixed T).

5. Magnetization

We define the reduced magnetization per vertex by

$$\mathscr{I}(K,\alpha) = I/N\mu = N^{-1}\partial \ln Z(K,L)/\partial L, \tag{27}$$

where I is the total magnetization of the lattice. The saturation value of the magnetization is given by $\mathscr{I} = \mathscr{I}_s = 2$. The transformation equations now yield

$$\mathscr{I}(K,\alpha) = (G_L)_K \mathscr{U}^*(G) + 2\partial \ln f(K,L)/\partial L. \tag{28}$$

In zero magnetic field both the derivatives $(G_L)_K$ and $\partial \ln f/\partial L$ vanish so that the magnetization is identically zero (as it should be). Figure 9 shows the behaviour of

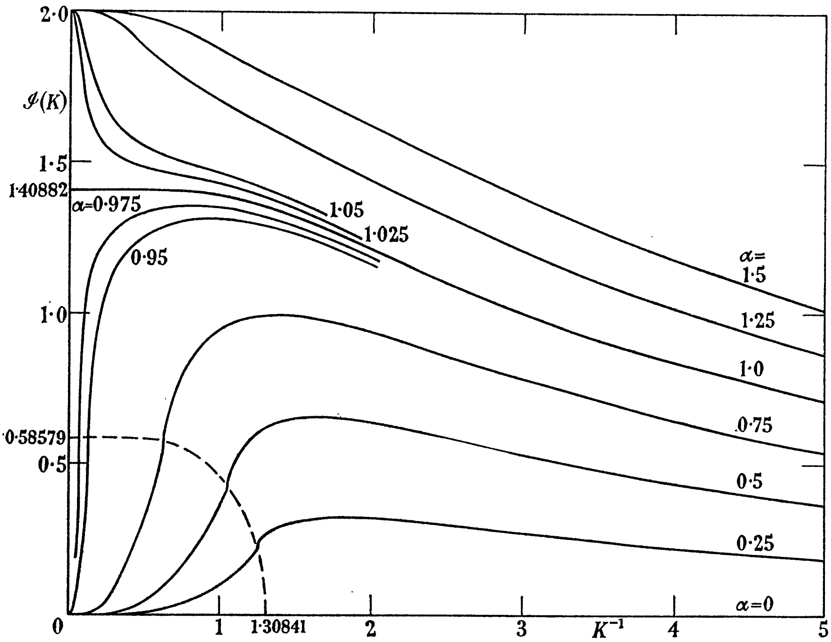

Figure 9. The magnetization versus temperature for fixed magnetic field. The value $\mathscr{I} = 2$ corresponds to saturation and the value $\alpha = 1$ corresponds to the critical magnetic field $H = H_c$. The dashed curve is the locus of transition points.

the magnetization as a function of temperature for fixed magnetic field. At high temperatures the magnetization falls to zero (according to Curie's law). As the temperature is reduced at a small fixed field ($\alpha < 1$) the magnetization rises and reaches a maximum at a temperature well above the appropriate transition temperature. With further decrease in temperature the magnetization falls sharply and in the transition region behaves as $\mathscr{I}_t + B(T_t - T)\ln|T_t - T|$, i.e. it is continuous and smoothly varying through T_t although, like the energy, it has an infinite temperature gradient at the transition point. This is at variance with the Bethe and similar approximations according to which the magnetization should show a 'kink', or discontinuous gradient at T_t. The dashed curve in figure 9 represents the locus of transition points, i.e. the curve of the transition magnetization $\mathscr{I}_t$ against temperature. As the temperature decreases to zero the curve becomes horizontal and intersects the axis at

$$\lim_{T\to 0} \mathscr{I}_t(T) = 2-\sqrt{2} = 0{\cdot}29289\mathscr{I}_s.$$

In the critical field H_c ($\alpha = 1$) the curve of magnetization displays no maximum (or other anomaly). However, at zero temperature it does *not* approach saturation, as might be expected. Rather, the mean magnetization at $T = 0$ and $H = H_c$ is given by

$$\lim_{T\to 0} \mathscr{I}_t(T, H_c) = \tfrac{3}{2} - \tfrac{1}{4}\mathscr{U}^*(\tfrac{1}{4}\ln 2) = 0{\cdot}70441\mathscr{I}_s.$$

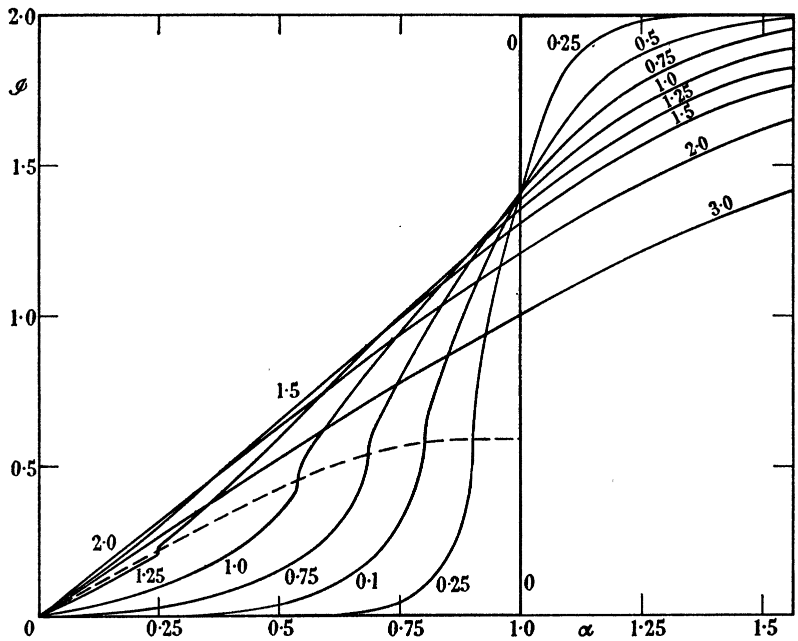

Figure 10. The magnetization as a function of magnetic field at fixed temperature. The dashed curve is the locus of transition points. The curves are labelled by the appropriate value of the reduced temperature K^{-1}.

For fields only slightly greater than H_c the magnetization exhibits a point of inflexion and increases very rapidly at low temperatures reaching saturation at $T = 0$ (see figure 9). At higher fields saturation is approached more gradually.

In figure 10 the magnetization is plotted against the field at constant temperature. Well above the critical point ($K^{-1} = 2{\cdot}0$ and $3{\cdot}0$) the curve is of standard paramagnetic type, i.e. concave downwards. Nearer the critical temperature (e.g. $K^{-1} = 1{\cdot}5$) the curve is concave upwards for small fields and exhibits a point of inflexion. Below the critical temperature the magnetization curve rises more sharply and at the transition field H_t displays an anomaly of the form

$$\mathscr{I}_t + B'(H_t - H)\ln|H_t - H|.$$

The dashed line represents the locus of transition points. At zero temperature the magnetization rises discontinuously to its saturation value at the critical field.

Figure 11 is a plot of the isomomentals in the temperature-field plane. The dashed line is the transition curve which is crossed *tangentially* by the isomomentals. It will be noticed that the isomomentals are appreciably curved in the paramagnetic region although the Bethe approximations predict that they should be straight (Ziman 1951).

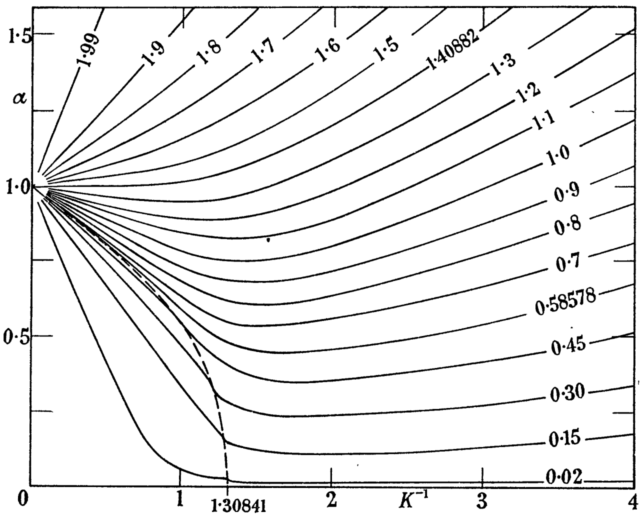

FIGURE 11. The contours of constant magnetization in the temperature-magnetic field plane. The dashed line is the transition curve.

6. SUSCEPTIBILITY

In experimental studies of the susceptibility χ it is customary to plot a graph of $1/\chi$ against T in order to effect a comparison with the Curie–Weiss law

$$[\chi \sim 1/(T+\theta)].$$

Antiferromagnets are characterized by a minimum in this curve, i.e. a maximum in the susceptibility χ. From the theoretical viewpoint, however, the quantity $T\chi$ is more significant than $1/\chi$. Accordingly we define† a 'specific susceptibility' by

$$\xi(K,\alpha) = kT\chi/N\mu^2 = N^{-1}\partial^2 \ln Z(K,L)/\partial L^2. \tag{29}$$

If Curie's law ($\chi \sim 1/T$) were obeyed ξ would be a constant (of value 2 in the present instance). Actually for an ideal antiferromagnet in zero field, $\xi(T)$ will fall monotonically as the temperature is decreased and will vanish at $T = 0$ (see figure 12). The transformation equations now yield

$$\xi(K,\alpha) = (G_{LL})_K\, \mathscr{U}^*(G) + (G_L)^2_K\, \mathscr{D}^*(G) + 2\,\partial^2 \ln f(K,L)/\partial L^2. \tag{30}$$

where $\mathscr{D}^*(G)$ is essentially the specific heat of the standard square Ising net. Explicitly

$$\mathscr{D}^*(G) = \frac{\partial^2}{\partial G^2} \ln Q(G) = \frac{\partial \mathscr{U}^*}{\partial G} = kT^{*2}C^*/J^2, \tag{31}$$

so that from Onsager (1944) we have

$$\mathscr{D}^*(G) = 2\coth^2 2G \left\{\frac{2}{\pi}K(k_1) - \frac{2}{\pi}E(k_1) - \tfrac{1}{2}(1-k_1'')\left[1 + k_1''\frac{2}{\pi}K(k_1)\right]\right\}, \tag{32}$$

† Other authors have also worked directly with this quantity.

where $$k_1'' = (1-k_1^2)^{\frac{1}{2}} = 2\tanh^2 2G - 1. \tag{33}$$

It can be seen that $\mathscr{D}^*(G)$ exhibits a logarithmic singularity at the critical point.

In zero magnetic field the derivative $(G_L)_K$ vanishes so that the singular term drops out of the expression for the specific susceptibility, which then simplifies to

$$\xi(K,0) = 2 - \tanh^2 2K\,[1+\tfrac{1}{2}\mathscr{U}^*(G)]. \tag{34}$$

In virtue of (23) and (26) this may also be written

$$\xi(K,0) = 2 - \tfrac{1}{2}\mathscr{U}(K,0)\tanh 2K, \tag{35}$$

which shows that the specific susceptibility (in zero field) is intimately connected with the corresponding configurational energy $\mathscr{U}(K,0)$. Figure 12 shows the

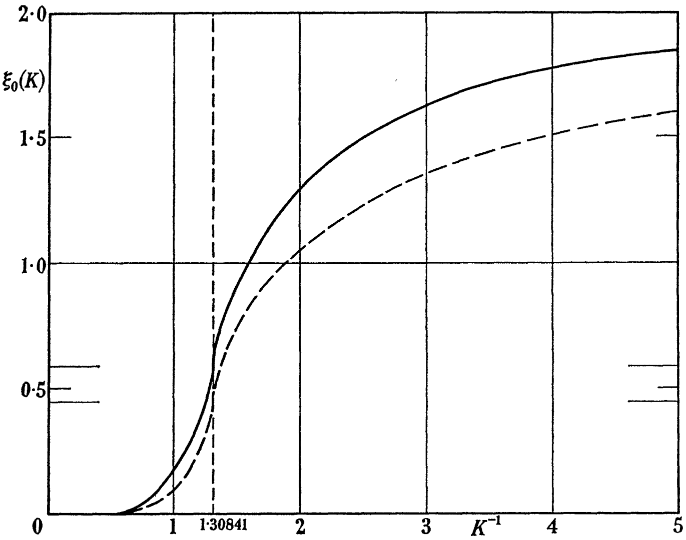

FIGURE 12. The zero-field specific susceptibility $\xi_0 = (k/N\mu^2)\,T\chi_0$ as a function of temperature (solid curve). The dashed curve represents $\frac{1}{2}[4-\mathscr{U}(K,0)]$, where $\mathscr{U}(K,0)$ is the reduced energy in zero field. The co-ordinates of the critical points are marked on the axes.

behaviour of $\xi(K,0)$ and that of $\frac{1}{2}[4-\mathscr{U}(K,0)]$ (dashed curve) for comparison. (It would be interesting to have similar experimental comparisons between $T\chi$ and the energy or between $\partial\chi/\partial T$ and the specific heat.) Clearly, the anomaly in ξ and hence in the initial (zero-field) susceptibility χ_0 is of the same type as that in the energy. In other words, in the transition region we have

$$\chi_0 \approx \frac{N\mu^2}{kT}\{\xi_c - D(T-T_c)\ln|T-T_c|\}, \tag{36}$$

where the critical value of the susceptibility per magnetic spin is determined by

$$\tfrac{1}{2}\xi_c = 1-\tfrac{1}{2}\sqrt{2} = 0{\cdot}29289.$$

The complete behaviour of the susceptibility is shown by the plot of $K\xi$ ($\sim \chi_0$) against temperature in figure 13 (solid curve). As T falls from high temperatures the susceptibility rises and reaches a maximum at a temperature of about $1{\cdot}40T_c$. As the critical temperature is approached χ_0 drops more sharply but is smoothly varying and continuous through the transition although $\partial\chi/\partial T$ becomes infinite at T_c. As noted in the Introduction this behaviour is at variance with almost all previous treatments of the problem.

Actually the author has shown (Fisher 1959*b*) that the relations (35) and (36) are special cases of a general result valid for antiferromagnetic plane Ising lattices. More precisely, by considering the spin-spin correlation functions it can be established that a relation of the type (35) between the specific susceptibility and the energy always holds. In the general case, however, the factor tanh $2K$ is replaced by some other, presumably more complicated, slowly varying function. For the standard Ising lattices a similar but somewhat less explicit formula had been obtained previously by Sykes & Fisher (1958) on the basis of combinatorial arguments.

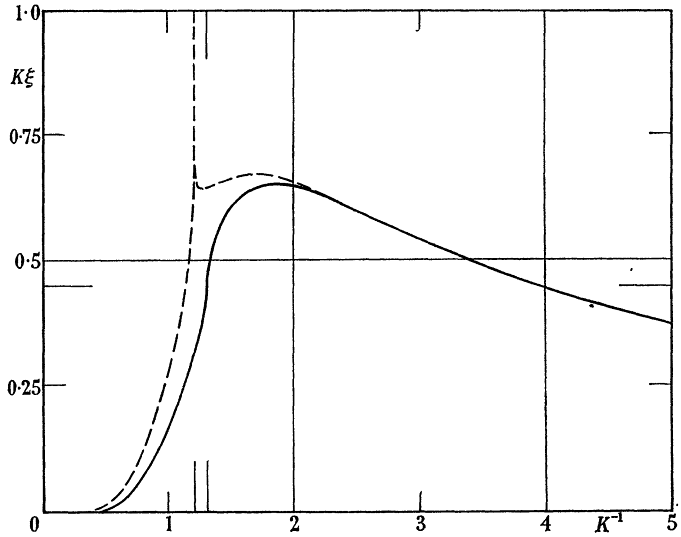

FIGURE 13. The temperature dependence of the zero-field susceptibility $\chi_0 \sim K\xi_0$ (solid curve) and the susceptibility in a magnetic field $H = \frac{1}{4}H_c$ (dashed curve). The critical co-ordinates are marked on the axes.

At high temperatures the susceptibility is given by the expansion

$$\chi_0 = \frac{2N\mu^2}{kT}\left\{1-2\left(\frac{J}{kT}\right)^2+\dots\right\}. \tag{37}$$

The first correction term to Curie's Law is of order $1/T^2$, whereas it is normally expected to be of order $1/T$. This difference is due directly to the 'super-exchange character' of the present model, i.e. to the fact that the magnetic spins are coupled to their neighbours *indirectly* via *two* bonds.

Although the susceptibility in zero field is finite at the transition temperature, this is no longer true in the presence of a magnetic field. The coefficient of the singular term $\mathscr{D}^*(G)$ in (30) has the expansion

$$(G_L)^2_K = \alpha^2K^2\tanh^4 2K + O(\alpha^4), \tag{38}$$

so that in a finite field the susceptibility has an infinity at the transition temperature. Near the critical point the behaviour is given by

$$\chi(T,H) \approx \frac{N\mu^2}{kT}\{\xi_c - D(T-T_c)\ln|T-T_c| - D'H^2\ln|T-T_c|\}, \tag{39}$$

which indicates that the magnitude of the singularity is proportional to the square of the field.

The dashed curve in figure 13 shows the behaviour of the susceptibility in a field $\alpha = \frac{1}{4}$. The position of the transition and of the maximum in χ have been shifted to lower temperatures and the height of the maximum has been increased. At this value of field the infinite peak at T_t is very narrow and to a rough approximation the transition appears rather as a discontinuity in gradient. This is reminiscent of many older experimental measurements (see, for example, the review article by Lidiard 1954) and of the predictions of the cruder theoretical treatments. It would be out of place to attempt a detailed comparison of the present model with experiment because of the obvious limitations of the dimensionality and the assumed Ising interaction. It is worth while, however, to point out that recent experiments on antiferromagnetic salts (for example, those by Lasheen *et al.* 1958 on $MnCl_2.4H_2O$ and by Cooke *et al.* 1959, on K_2 Ir Cl_6) bear out the general behaviour shown in figure 13. Thus it is found that the maximum in χ occurs above† the transition point (Neél temperature) which in turn is characterized by an exceedingly sharp drop in χ coincident with the specific heat anomaly. Furthermore, differential measurements of χ in a finite field clearly indicate a lowered transition temperature, an increased height and lower temperature for the maximum and a quadratic dependence on the magnetic field. So far measurements in a finite field have been too coarsely spaced to reveal the possible existence of a small peak in χ at the transition temperature. It would be interesting to have more detailed experiments.

7. Conclusions and generalizations

We have studied the exact behaviour of the thermodynamic and magnetic functions of a particular two-dimensional model of an antiferromagnet in an arbitrary magnetic field. The corresponding long-range and short-range order or spin pair correlations may also be evaluated and this is done in part II of the present paper.

The model investigated is only one of a number of similar exactly soluble antiferromagnetic lattices. A simple generalization is the introduction of second-neighbour interactions between the non-magnetic vertex spins of the model. This leads to a series of models which display a variety of interesting features. Furthermore, all these lattices can still be solved exactly if the magnetic spins have an arbitrary magnitude S. Other models can be found in which coupling between the magnetic spins in one lattice direction is direct (rather than indirect as is the

† The maximum in the case of $MnCl_2.4H_2O$ occurs only about 5 % above T_c as against 40 % on our model. Comparison with series expansions for the three-dimensional Ising model suggests that this difference is essentially due to the lower dimensionality of the model. Most critical phenomena appear to set in more sharply in three dimensions than in two.

'super-exchange' coupling of the present model). The author hopes to discuss some of these models in the future.

It is clear that similar models could be constructed in three dimensions. Thus if the simple cubic Ising lattice could be solved in zero magnetic field one would have a three-dimensional model of an antiferromagnet soluble in an arbitrary magnetic field. As in two dimensions the behaviour of the initial susceptibility in the transition region would match the anomaly in the energy. The approximate work that has been performed on the simple cubic lattice (by extrapolating precise series expansions (see, for example, Wakefield 1951)) does enable us to conclude, for example, that the susceptibility would show the same general features as in figure 13. The exact nature of the anomalies, however, cannot at present be predicted.

As is well known (see, for example, Newell & Montroll 1953) the standard Ising model of antiferromagnetism is equivalent to the order-disorder problem for a binary alloy and to a lattice gas with repulsive interactions. (The latter model has been studied recently by Burley 1959 and by Temperley 1959.) The restriction to zero magnetic field (and hence zero magnetization) corresponds for these models to stoichiometric composition ($N_A = N_B$) and fixed density ($\rho = \frac{1}{2}\rho_{\text{max.}}$), respectively. This restriction is removed by the present model but the 'super-exchange' coupling leads to an additional temperature-dependent four-body interaction which is rather artificial. None the less, certain predictions may be of general significance.

The present model and its generalizations should be useful for testing the predictions of approximate methods in a finite magnetic field. Hitherto this has only been possible for zero field.

Finally, we consider how far the properties of the 'super-exchange' antiferromagnetic lattices will be representative of the properties of the standard antiferromagnetic Ising lattices. This question cannot, at present, be answered with complete rigour, but it seems probable that in all essential features the models will agree. Thus in zero field the anomalies in the thermodynamic functions, and also (as will be shown in part II) in the long-range order and in the correlations, are certainly the same as displayed by the standard plane lattices. Furthermore, as mentioned above, one can show (Fisher 1959*b*) that the anomalies in the initial susceptibilities also agree. This implies that the magnetizations, at least in small fields, behave in the same way which, in turn, indicates that the susceptibilities in a magnetic field will exhibit similar singularities. Indeed, it emerges generally from the study of co-operative phenomena (see, for example, Domb & Sykes 1956 and Rushbrooke & Wood 1958) that for a given type of interaction the nature of the transition anomalies depends primarily on the dimensionality of the lattice and there seems little reason to suppose this is not also true in a magnetic field.

The author is grateful to Professor C. Domb and to Dr M. F. Sykes for their comments on the manuscript and for stimulating discussions.

References

Anderson, P. W. 1950 *Phys. Rev.* **79**, 350.
Brooks, J. E. & Domb, C. 1951 *Proc. Roy. Soc.* A, **207**, 343.
Burley, D. M. 1959 Ph.D. thesis, London.
Cooke, A. H., Lazenby, R., McKim, F. R., Owen, J. & Wolf, W. P. 1959 *Proc. Roy. Soc.* A, **250**, 97.
Domb, C. & Potts, R. B. 1951 *Proc. Roy. Soc.* A, **210**, 125.
Domb, C. & Sykes, M. F. 1956 *Proc. Roy. Soc.* A, **235**, 247.
Domb, C. & Sykes, M. F. 1957 *Proc. Roy. Soc.* A, **240**, 214.
Fisher, M. E. 1959*a* *Phys. Rev.* **113**, 969.
Fisher, M. E. 1959*b* *Physica*, **25**, 521.
Houtappel, R. M. F. 1950 *Physica*, **16**, 425.
Kaufman, B. & Onsager, L. 1949 *Phys. Rev.* **79**, 350.
Kikuchi, R. 1951 *Phys. Rev.* **81**, 988.
Kubo, R., Nagamiya, T. & Yosida, K. 1955 *Advanc. Phys.* **4**, 1.
Lasheen, M. A., van den Broek, J. & Gorter, C. J. 1958 *Physica*, **24**, 1061, 1076.
Lidiard, A. B. 1954 *Rep. Progr. Phys.* **17**, 201.
Naya, S. 1954 *Progr. Theor. Phys. Osaka*, **11**, 53.
Newell, G. F. & Montroll, E. W. 1953 *Rev. Mod. Phys.* **25**, 353.
Onsager, L. 1944 *Phys. Rev.* **65**, 117.
Park, D. 1956 *Physica*, **22**, 932.
Rushbrooke, G. S. & Wood, P. J. 1958 *Mol. Phys.* **3**, 257.
Shull, C. G. & Smart, J. S. 1949 *Phys. Rev.* **76**, 1256.
Sykes, M. F. & Fisher, M. E. 1958 *Phys. Rev. Letters*, **1**, 321.
Syozi, I. 1951 *Progr. Theor. Phys. Osaka*, **6**, 306.
Syozi, I. & Nakano, H. 1955 *Progr. Theor. Phys. Osaka*, **13**, 69.
Temperley, H. N. V. 1959 *Proc. Phys. Soc.* **74**, 183.
Wakefield, A. J. 1951 *Proc. Camb. Phil. Soc.* **47**, 799.
Yang, C. N. 1952 *Phys. Rev.* **85**, 808.
Ziman, J. M. 1951 *Proc. Phys. Soc.* A, **64**, 1108.